Mat. Res. Soc. Symp. Proc. Vol. 716 © 2002 Materials Research Society

Near-Field Ultrasonic Imaging: A Novel Method for Nondestructive Mechanical Imaging of IC Interconnect Structures

G. S. Shekhawat, H. Xie, Y. Zheng, and R. E. Geer
University at Albany Institute for Materials, Albany, NY 12222

ABSTRACT

The investigation of an alternate approach to nondestructive, nanoscale mechanical imaging for IC interconnect structures is reported. This approach utilizes a heterodyne interferometer based on a scanning probe microscope, also referred to as heterodyne force microscopy (HFM). This interferometer is sensitive to the relative phase difference of the two ultrasonic excitations due to spatial variations in the sample viscoelastic response and enables near-field, phase-sensitive imaging. Proof-of-feasibility demonstrations of this technique are presented for ultrasonic phase-imaging of Al/low-k interconnect structures. Spatial resolution < 10 nm is demonstrated.

INTRODUCTION

Spatial resolution limitations restrict the application of conventional ultrasonic or acoustic imaging to integrated circuit (IC) structures. Simply, the spatial resolution, *w*, of an acoustic microscope is given by [1]:

$$w = 0.51\frac{v_o}{fN.A.}$$

where v_o is the speed of sound in the coupling medium, f is the frequency of the acoustic/ultrasonic wave, and *N.A.* is the numerical aperature of the lens. For a frequency of 1 GHz the nominal spatial resolution attainable is approximately 1.5 μm.

Higher resolution alternatives for nondestructive mechanical imaging include the atomic force microscope (AFM) or scanning probe microscope (SPM) platforms. Force modulation microscopy (FMM) [2], ultrasonic-AFM [3], ultrasonic force microscopy (UFM) [4] are a few examples. Each technique is traditionally sensitive to the static elastic properties of the sample surface. Recently, a high spatial resolution phase-sensitive technique has been demonstrated which employs an ultrasonic heterodyne methodology for imaging elastic as well as viscoelastic variations across a sample surface [5]. So-called heterodyne force microscopy (HFM) uses a near-field approach to measure time-resolved variations in ultrasonic oscillations at a sample surface. As such, it holds potential for overcoming the spatial resolution limitations of conventional phase-resolved acoustic microscopy (i.e. holography) by eliminating the need for far-field acoustic lenses. The work presented here investigates the application of HFM at low carrier frequencies (2.2 MHz) to IC interconnect test structures consisting of a 1-level Al/low-k polymer damascene wiring pattern to evaluate potential metrology applications for surface and subsurface nanomechanical imaging. Initial results reveal the high mechanical and viscoelastic image contrast capable with HFM on such structures. In addition, the variation of the viscoelastic phase with HFM operational parameters is also evaluated and indicates a strong, nonlinear relationship to sample and tip ultrasonic vibration amplitudes.

HFM OPERATIONAL PRINCIPLES

In conventional UFM the super-resonant vibration of the sample substrate results in a deflection, z_c, of the SPM cantilever related directly to the elastic/adhesive properties of the

sample if the vibration amplitude is sufficient to probe the nonlinear region of the tip/sample force-displacement curve, *F(h)* [6]. This defleciton is summarized mathematically below.

$$\langle F(h_o, A)\rangle = \frac{\omega}{2\pi}\int_0^{2\pi/\omega} F(h_o - A\cos(\omega t)dt = k_c z_c$$

k_c is the cantielver spring constant, A is the sample vibration amplitude and ω the oscillation frequency. In HFM, a second ultrasonic oscillation is applied to the cantilevered tip. The excitation of higher order flexural modes within the cantilever structure provides a super-resonant vibration of the tip. The resulting cantilever deflection can now be represented as:

$$\langle z(\omega_{TIP}, \omega_S, A_{TIP}A_S) - z_o\rangle \propto \int \Delta F(Z_{TIP} - Z_S)dt$$
$$= \int dt\chi_1(Z_{TIP} - Z_S) + \chi_2(Z_{TIP} - Z_S)^2 + ...$$

where z_o is the static (zero frequency) position of the tip, $\Delta F(Z_{TIP}\text{-}Z_S)$ refers to the variation of the tip/sample force from its static value, $Z_S = A_S\cos(\omega_S t + \omega_S\tau)$, and $Z_{TIP} = A_{TIP}\cos(\omega_{TIP}t + \varphi_{TIP})$. Here, τ is a relaxation time or phase delay time associated with the surface vibration resulting from a time-dependent mechanical process within the material. φ_{TIP} is an arbitrary constant phase associated with the tip vibration. The heterodyne nature of this deflection is illustrated by assuming a weak nonlinearity represented by a nonvanishing 2nd order susceptibility, χ_2, above. Assuming that the high-frequency response of the cantilever vibrations is beyond the temporal resolution of the SPM photodiode, the average deflection is simply calculated to be [5]:

$$\langle z(\omega_{TIP}, \omega_S, A_{TIP}A_S) - z_o\rangle = \chi_2\left\{\frac{A_{TIP}^2}{2} - A_{TIP}A_S\cos[(\omega_{TIP} - \omega_S)t - \omega_S\tau + \varphi_{TIP}] + \frac{A_S^2}{2}\right\}.$$

The heterodyne amplitude and phase are experimentally extracted from the tip deflection signal via conventional lockin detection. The phase sensitivity of this measurment is critical in extracting time-resolved mechanical properties of materials as well as potentially enabling subsurface imaging. It is important to note that in practice the oscillation amplitudes used for HFM are sufficiently large such that the simplistic 2nd order approximations made above are not valid. More detailed modeling is required to include more complex higher order couplings and is currently underway.

EXPERIMENTAL

A conventional JEOL SPM 4200 scanning probe microscope system was modified to operate in the HFM mode. Commercial piezoelectric ceramics were used to provide ultrasonic vibrations to the tip and sample. Each possessed an out-of-plane resonance at approximately 2.2 MHz. Matching piezoceramics were required to keep the frequency difference below the cutoff frequency of the SPM photodiode (~ 600 kHz). Two function generators were used to drive each piezoceramic. A simple mixing circuit was used to extract the heterodyne frequency which was used as a reference to an RF lockin amplifier. The SPM differential photodiode signal constituted an input to this lockin. The resultant heterodyne amplitude and phase images were acquired using the standard raster electronics of the SPM controller.

RESULTS AND DISCUSSION

Single-level damascene IC test structures were used to evaluate the static and viscoelastic imaging of HFM. These consisted of thermal chemical vapor deposited (CVD) aluminum in a reactive-ion-etched (RIE) patterned matrix of benzocyclobutene polymer deposited on a 200mm

silicon (100) wafer. The fabrication of this test structure and its investigation via conventional UFM has been described previously [7]. The region of interest for these investigations comprise an array of polymer plugs inlaid within an Al matrix (schematically depicted in Fig. 1). The plugs varied between 1.5 μm and 2.0 μm on a side and extend to a depth of 700 nm. Three sets of mechanical images for this test structure are shown in Fig. 1. The top row is comprised of topography scans taken simultaneously with the corresponding elastic/viscoelastic scan shown in the bottom row. From the topography scans the polymer plugs extend above the surrounding Al due to its reduced planarization rate compared to Al. Accepted elastic moduli for Al is approximately 68 GPa and for the benzocyclobutene polymer is approximately 4 GPa [7].

Figure 1c shows a conventional UFM image and the corresponding topography of the Al/polymer test structure. In these materials the image contrast is directly proportional to the material elastic constant and has been reported previously. Figure 1a shows the image associated with the HFM amplitude signal (bottom) and the simultaneously recorded topography (top). Qualitatively, the HFM amplitude and the UFM image are extremely similar. The HFM phase image is shown in Fig. 1b. This data is collected simultaneously with the HFM amplitude image. Qualitatively, the HFM phase image is similar in contrast variation with the amplitude image. This is expected considering the lower modulus and higher loss tangent associated with the polymer in comparison with the Al. The minimum relative viscoelastic phase variation detectable in this image is approximately 0.025v that, assuming a direct relationship with the carrier frequency (2.2 MHz), corresponds to a phase delay of approximately 570 ps. Spatial resolution was also evaluated and determined to be approximately 10 nm.

Increased magnification images of the HFM amplitude and phase variation of the polymer regions are shown in Fig. 2. Note the Amp-HFM image contrast over the polymer plug is essentially constant. However, the Ph-HFM image contrast (i.e. viscoelastic delay of the surface vibration) across the polymer varies markedly near the Al interface (this region is denoted by arrows in the Ph-HFM image). This region is interior to the polymer plug and varies in width from 350nm to 190nm. The presence of this contrast in the Ph-HFM image but not the Amp-HFM image implies the interfacial region possesses a distinct viscoelastic response compared to the interior of the polymer plug. This is a very important result in that a portion of

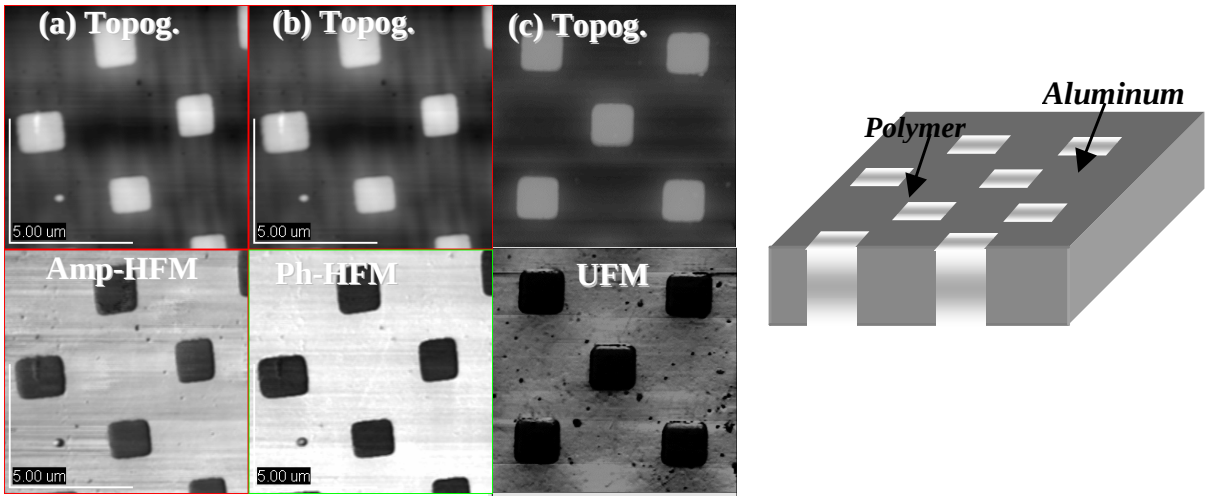

Figure 1 (a) Topography and HFM amplitude images. (b) Topography and HFM phase images. (c) Topography and conventional UFM images. All scans are 10 μm x 10 μm. Right: Schematic of Al/polymer test structure. Polymer plugs are ~ 2μm x 2μm.

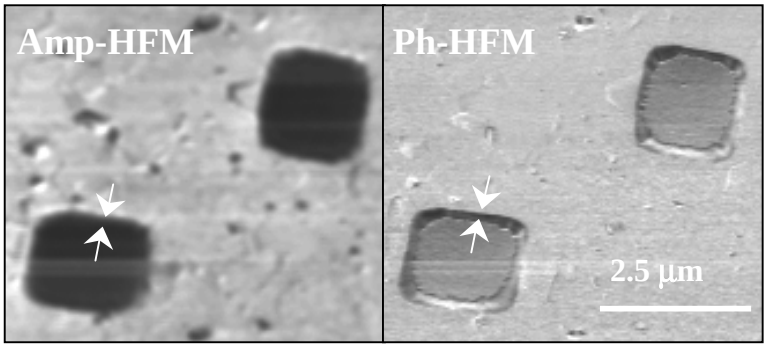

Figure 2 Higher magnification Amp-HFM and Ph-HFM images of the Al/polymer test structures. Note the appearance of a distinct Al/polymer boundary region in the Ph-HFM that is absent in the Amp-HFM image (white arrows). This region exhibits a distinct dynamic response time possibly resulting from process-induced variations in the polymer.

the polymer, although elastically uniform, possesses a modified visoelastic response. Although the origin of the variation in the viscoelastic phase delay is unknown at this time it has already been shown that vapor phase processing can induce significant compositional and mechanical variations in this polymer [8]. Such a root cause may also be present here. The polymer plugs are formed by subtractive etching wherein the top side of the plug is covered by an SiO_2 hardmask [9]. The Al is subsequently deposited via CVD and the excess Al and hardmask is removed via planarization. The exposure of the polymer plug sidewall to the RIE and CVD Al processing (while the top side is protected by the SiO_2 hardmask) may alter the dissipative (hence viscoelastic) properties of the polymer without necessarily changing the static polymer modulus.

The quantification of this phase variation is of significant interest if it is to be used to extract material properties or exploited for subsurface mechanical imaging. Figure 3 shows the variation of the HFM phase image with increasing voltage. Clearly, the relative phase contrast between the polymeric and Al regions varies strongly with sample vibration amplitude (given arbitrarily in terms of the driving voltage). This variation contradicts the oversimplified cantilever deflection calculation presented above. Two primary causes for the amplitude dependent phase are: (a) The viscoelastic response (and hence phase delay) may be inherently nonlinear at oscillation amplitudes necessary to probe the nonlinear region of the tip/sample force-displacement curbe; (b) The spatial variation of the tip-dependent phase term related to the resonance spectra of the cantilever and the mechanical coupling to the sample. The former can be probed simply by varying the sample vibration amplitude. Assuming an intertially damped cantilever, the increased excursion of the tip along the force-displacement curve would increase monotonically with applied voltage. Inherently linear viscoelastic response would intuitively provide a constant relative phase delay as a function of voltage. The second panel of Fig. 3 also plots the observed phase delay between the polymeric and Al regions as a function of applied sample piezo amplitude (volts). The tip piezo amplitude was held constant at 2.0v. The increase is approximately monotonic which implies a nonlinear viscoelastic response, or a strongly varying coupling between the tip and sample which shifts the heterodyne oscillation [5]. The operational parameters of the piezoelectric ceramics used here restricts the voltage to values below 10v to prevent damage. Although not conclusive, the data in Figs. 2-3 certainly imply a novel dynamic imaging mechanism associated with HFM that is relevant for IC structures.

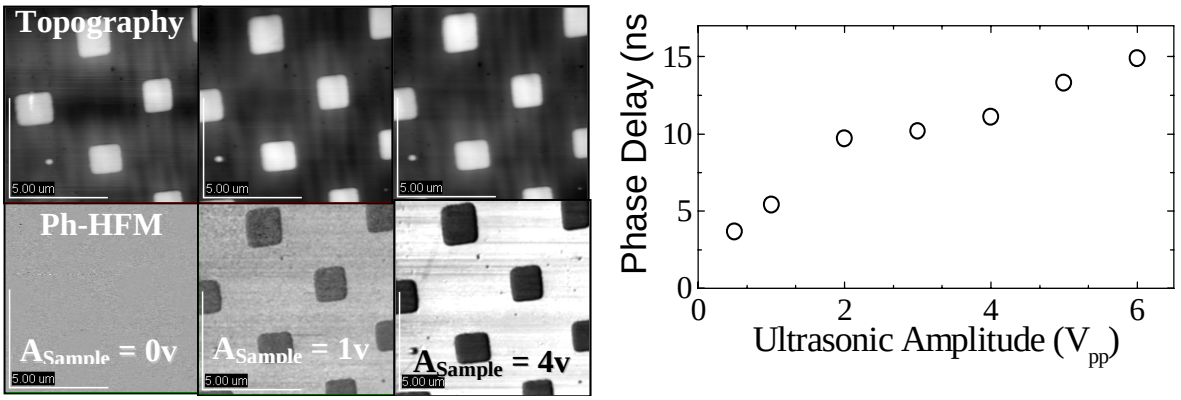

Figure 3 Left: Topography (top) and Ph-HFM images (bottom) of the test structure at selected values of the sample piezo driving voltage. An apparent increase in phase delay differential between the Al and the polymer with increasing sample piezo amplitude is evident. Right: Plot of relative phase delay between the Al and the polymer regions of the sample as a function of the sample piezo driving voltage.

The second possible source of phase variation with ultrasonic amplitude noted above was investigated by a simple matrix of sample and tip vibration amplitudes. Without a detailed calibration of the tip vibration response function its amplitude is assumed to respond as a simple forced oscillator and increase linearly with driving voltage. The 3-dimensional plot of relative phase delay between the polymeric and Al regions is shown in Fig. 4. The most pronounced feature of this plot is the clear maximum in relative phase difference at a tip vibration driving voltage of approximately 4 volts. The FWHM of the this peak decreases with increasing sample vibration amplitude. In contrast, the relative phase delay between the Al and polymeric regions is an approximately monotonic function of sample vibration amplitude. Initial testing indicates that the strong peak as a function of tip-piezo driving voltage results from the combination of two

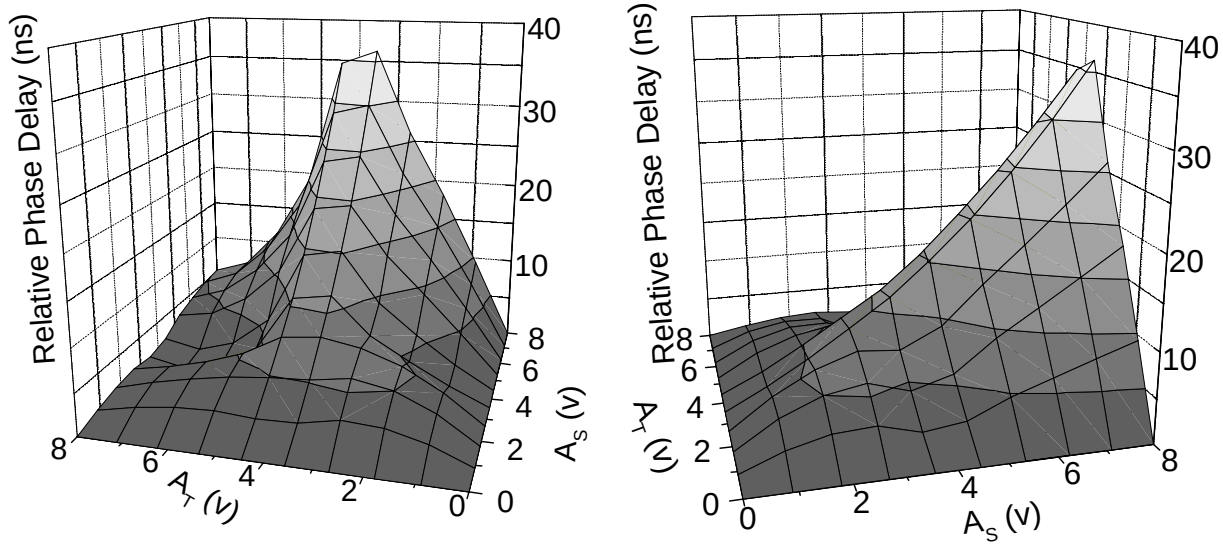

Figure 4 Two perspectives of a 3-dimensional plot of relative phase-delay between the Al and polymer components from Ph-HFM images as a function of both tip piezo driving voltage and sample piezo driving voltage.

factors. Firstly, variation in the amplitude results in a change in the average tip/sample force and slightly shifts the resonance frequency of the cantilever. This shift can result in an overall drop in piezo oscillation amplitude as well as shifting the cantilever phase (φ_{TIP}). A drop in the amplitude of the tip oscillation amplitude may also result in a decrease in possible nonlinearities in the viscoelastic response function of the material. Hence the peak along the A_{TIP} axis reflects the cantilever flexural resonance spectrum. Since the sample oscillation resonances do not exhibit such sensitivity, the variation along the A_S axis is presumably dominated by the sample viscoelastic response.

CONCLUSION

The investigation of an alternate approach to nondestructive, nanoscale mechanical imaging for IC interconnect structures is reported. Preliminary studies of HFM have demonstrated the ability to measure, with high spatial resolution, the viscoelastic response of an Al/polymer IC test structure. Spatial resolution < 10 nm was demonstrated. A vibrational amplitude dependence of the viscoelastic phase delay was observed. This behavior was attributed to an inherent nonlinearity in the sample viscoelastic response with increasing tip impingement in addition to a resonance-induced amplitude variation within the cantilever tip.

ACKNOWLEDGEMENTS

The authors gratefully acknowledge support from the Microelectronics Advanced Research Corporation and the New York State Office for Science, Technology, and Academic Research. It is a pleasure to acknowledge J. Hummel and J. Liu for assistance in test structure fabrication and characterization.

References

[1] G. A. D. Briggs, Acoustic Microscopy, (Clarendon Press, Oxford, 1992) p. 28.
[2] P. Maivald, H. J. Butt, S. A. C. Gould, C. B. Prater, B. Drake, J.A. Gurley, V. B. Elings, and P. K. Hansma *Nanotechnology* **2,** 103 (1991).
[3] U. Rabe and W. Arnold, *Appl. Phys. Lett.* **64,** 1423 (1994).
[4] O. V. Kolosov, K.Yamanaka, *Jpn. J. Appl. Phys.* **32**, 1095 (1993).
[5] M. T. Cuberes, H. E. Assender, G. A. D. Briggs and O. V. Kolosov, *J. Phys. D: Appl. Phys.* **33,** 2347 (2000).
[6] F. Dinelli, M. R. Castell, D. A. Ritchies, N. J. Mason, G. A. D. Briggs, and O. V. Kolosov, *Philosophical Magazine A* **80**, 2299 (2000).
[7] R. E. Geer, O.V. Kolosov, G.A.D. Briggs, and G. S. Shekhawat, *J. of Appl. Phys.*, in press.
[8] S. A. Vitale, H. Chae, and H. H. Sawin, *J. Vac. Sci. Technol*. **A18**, 2770 (2000).
[9] Heidi Gundlach, Robert Talevi, Zailong Bian, Guillermo Nuesca, Sujatha Sankaran, Kaushik Kumar, Alain E. Kaloyeros, Robert E. Geer, Joyce Liu, John Hummel, Edward O. Shaffer and Steven J. Martin, *J. Vac. Sci. Technol.*, **B18**, 2463 (2000).